

Cite this: *New J. Chem.*, 2011, **35**, 2136–2145

www.rsc.org/njc

PAPER

Electronic structure and metal–metal communication in $(\text{CpM})_2(\text{as-indacene})$ and $(\text{CpM})_2(\text{s-indacene})$ ($\text{M} = \text{Mn}, \text{Fe}, \text{Co}, \text{Ni}$) complexes: a DFT investigation†

Maria Teresa Garland,^a Samia Kahlal,^{bc} Desmond Mac-Leod Carey,^d
Ramiro Arratia-Pérez,^d Juan Manuel Manríquez^e and Jean-Yves Saillard^{*bc}

Received (in Victoria, Australia) 15th March 2011, Accepted 12th May 2011

DOI: 10.1039/c1nj20240e

DFT calculations with full geometry optimization have been performed on the series $(\text{CpM})_2(\text{as-indacene})$ and $(\text{CpM})_2(\text{s-indacene})$ ($\text{M} = \text{Mn}, \text{Fe}, \text{Co}, \text{Ni}$), as well as on the cations of the Fe, Co and Ni complexes. The compounds where $\text{M} = \text{Fe}$ and Ni (*as-indacene* series) and $\text{M} = \text{Mn}, \text{Fe}$ and Co (*s-indacene* series) were found to possess closed-shell ground states. In the mixed-valent cations as well as in the other open-shell species, the degree of metal–metal communication and the participation of the ligand into the spin density were evaluated. In general, the larger the total electron number, the larger the metal–metal communication and ligand participation to the frontier orbitals.

Introduction

Binuclear transition-metal complexes in which the two metal centers are connected through a conjugated organic linker are the subject of huge interest in coordination chemistry, owing to their various potential physical properties associated with the nature of the electronic communication between the metal centers.¹ From this point of view, conjugated fused polycyclic ligands offer the possibility of coordinating two (or more) metal moieties, often giving rise to stable isolable species which additionally can exhibit interesting redox behavior. Dinuclear complexes of indacene (*as*- or *s*-) constitute one of the largest family of this type of complexes, many of them having been structurally characterized.^{2–10} In this paper we investigate by the means of DFT calculations (see computational details) the coordination mode and the electronic structure of a series of $(\text{CpM})_2(\text{Ic})$ ($\text{M} = \text{Mn}, \text{Fe}, \text{Co}, \text{Ni}$; $\text{Ic} = \text{indacene}$) complexes and of some of their cations. Although this work is not the first theoretical investigation of dinuclear indacene complexes,^{9–15}

it is to our knowledge the first comprehensive DFT study of an homogeneous series of homonuclear compounds in which the monotonous variation of the number of electrons is the major parameter determining the differences in the molecular structures and metal–metal communication. Indeed, apart from one general qualitative investigation at the semi-empirical level published some years ago by our group,¹¹ the other theoretical studies were focussed on specific compounds and did not consider the indacene coordination chemistry from the point of view of the structure/electron count/properties relationships. On the other hand, experimental data on a series of complexes related to those investigated in this paper exist, namely compounds of the type $(\text{Cp}^*\text{M})_2(\text{Ic})$ ($\text{Cp}^* = \text{C}_5\text{Me}_5$), including physical properties of their mixed valent cations.

The *as*-indacene and *s*-indacene ligands

The free *as*-Ic and *s*-Ic molecules are antiaromatic systems (12 π -electrons) and therefore rather unstable species. When coordinated to metals, they are generally in their formal dianionic state and thus should be considered as aromatic (14 π -electron) indacenediide ligands. Their major resonant Lewis formulae are given in Scheme 1. Assuming that a dinuclear complexation occurs only at the C_5 rings, it appears from Scheme 1 that *as*-Ic^{2−} can provide a maximum of $2 \times 6 = 12$ π -electrons to the metal centers (formula **I**(*as*)), whereas *s*-Ic^{2−} is a potential donor of only $4 + 6 = 10$ π -electrons (see **I**(*s*) and **I'**(*s*)) unless the formulae **III**(*s*), **III'**(*s*) or **IV**(*s*) are considered to have significant statistical weights, despite the fact that they do not satisfy the octet rule. These latter formulae are associated with non-bonding $2p_\pi$ AO's of C(4) and C(8) and differ only by the fact that the two former

^a Laboratorio de Cristalografía, Departamento de Física, Facultad de Ciencias Físicas y Matemáticas, Universidad de Chile, Avenida Blanco Encalada 2008, Santiago, Chile

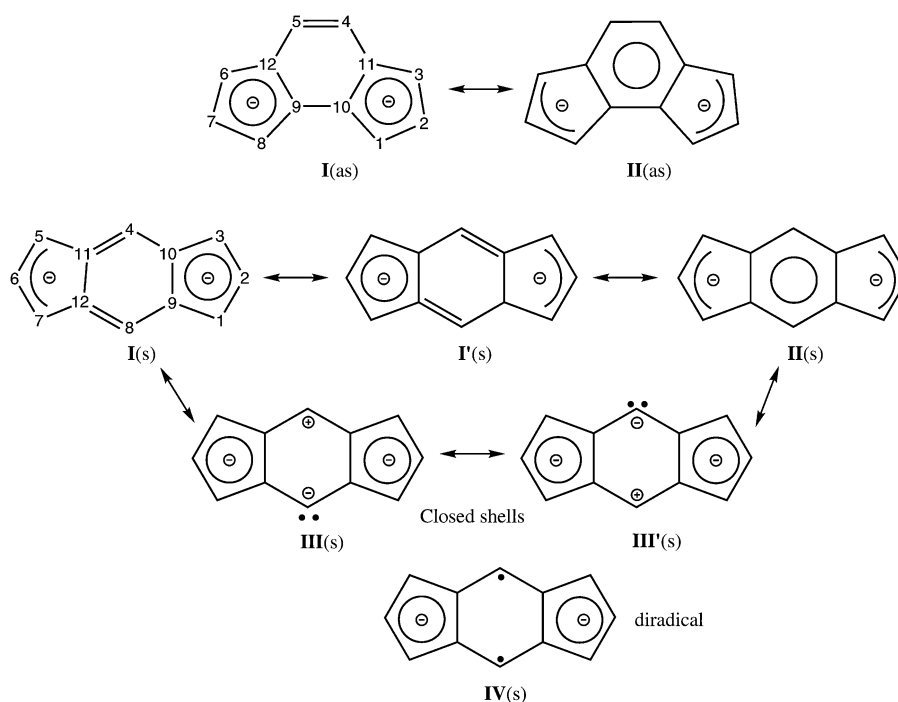
^b UMR 6226 Sciences Chimiques de Rennes, CNRS-Université de Rennes 1, Campus de Beaulieu, 35042 Rennes-Cedex, France. E-mail: saillard@univ-rennes1.fr

^c Université Européenne de Bretagne, 5 bd Laënnec, 35000 Rennes, France

^d Departamento de Ciencias Químicas, Relativistic Molecular Physics (ReMoPh) group, Universidad Andrés Bello, República 275, Santiago, Chile

^e Facultad de Químicas, Pontificia Universidad Católica de Chile, Casilla 306, Correo 22, Santiago, Chile

† This paper is dedicated to an outstanding chemist, our friend Didier Astruc, on the occasion of his 65th birthday.



Scheme 1 Major Lewis structures of *as*-Ic²⁻ and *s*-Ic²⁻ with the atom labeling used throughout this paper.

describe a closed-shell situation while the third one is a diradical. They confer to *s*-Ic²⁻ the potentiality to be a 12 π -electrons donor. Thus, in contrast to *as*-Ic²⁻, *s*-Ic²⁻ is ambivalent with respect to the maximum number of π electrons it can donate to the metals. This point will be analyzed in more details below.

The π MO diagrams computed at the BP86 level (see computational details) of the free *as*-Ic²⁻ and *s*-Ic²⁻ ligands are depicted in Fig. 1. The HOMO and LUMO of *s*-Ic²⁻ can be approximately described as deriving from the out-of-phase and in-phase combinations of the 2p $_{\pi}$ AO's of C(4) and C(8), respectively. This would suggest significant participation of the **III**(*s*) and **III'**(*s*) formulae of Scheme 1, if significant admixture of other carbon 2p $_{\pi}$ AO's into both the HOMO and LUMO would not induce the existence of a rather large gap between them (1.86 eV). Consistently, the corresponding triplet state (see **IV**(*s*) in Scheme 1) is computed to lie 1.70 eV (39.2 kcal mol⁻¹) higher in energy. Thus, the statistical weights of formulae **III**(*s*), **III'**(*s*) and **IV**(*s*) have to be considered very small in free *s*-Ic²⁻. However, they could become more important upon coordination to transition metals. The HOMO/LUMO gap of *as*-Ic²⁻ (2.39 eV) is larger than that of *s*-Ic²⁻, indicating greater stability. Consistently, the total energy of *as*-Ic²⁻ is computed to be lower than that of *s*-Ic²⁻ by 0.71 eV (16.4 kcal mol⁻¹).

(CpM)₂(*as*-Ic) complexes

Two different molecular configurations are possible, depending on the fact that both MCp moieties lie on the same side of the indacene plane (*syn*) or on different sides (*anti*). The geometry optimization of both *syn* and *anti* configurations of the neutral (CpM)₂(*as*-Ic) (M = Mn, Fe, Co, Ni) complexes has been

performed at the BP86 level (see computational details below), considering that the metal atoms coordinate the C₅ rings, as usually observed experimentally. For obvious sterical reasons, the *anti* configuration was always found to be slightly more stable than the *syn* configuration. Because the electronic structures of the *syn* and *anti* configurations were found to be very similar, only the data corresponding to the *anti* isomers are provided below, along with the *syn/anti* energy difference. The major computed data and the corresponding MO diagrams (singlet states) of the optimized *anti*-(CpM)₂(*as*-Ic) complexes are provided in Table 1 and Fig. 2, respectively. In the following, the electron richness of the whole molecule is defined as its total number of electrons (TNE) which is the sum of the π electrons of the ligands (*i.e.* 14 for Ic²⁻ and 6 for Cp⁻) and the M(II) valence electrons (assuming a neutral molecule). That is, TNE = 14 + 2 \times 6 + 2 \times (*n* - 2) = 22 + 2*n* if *n* is the valence electron number of M(0). One should note that TNE is not necessarily equal to the number of electrons effectively lying in the coordination spheres of the metals (MVE = metal valence electron number), since all the π -electrons of ligands are not necessarily donated to the metals. Thus, MVE \leq TNE and MVE is likely not to be very different from the favored 2 \times 18 = 36 count.

We start the analysis with the more straightforward case of M = Fe (TNE = 38) which can be considered as made of two coupled ferrocenic units. The C₅ rings of the indacene ligand are coordinated to the metals in a regular pentahapto coordination mode. The computed HOMO/LUMO gap (1.93 eV) is the largest of the series, in agreement with the existence of two stable ferrocenic 18-electron metal centers (MVE = 2 \times 18 = 36). Our results are in a very good agreement with the experimental structure and the diamagnetic behavior of *anti*-[Cp*Fe₂(*as*-Ic)] (Cp* = η^5 -C₅Me₅).⁵ Other diamagnetic

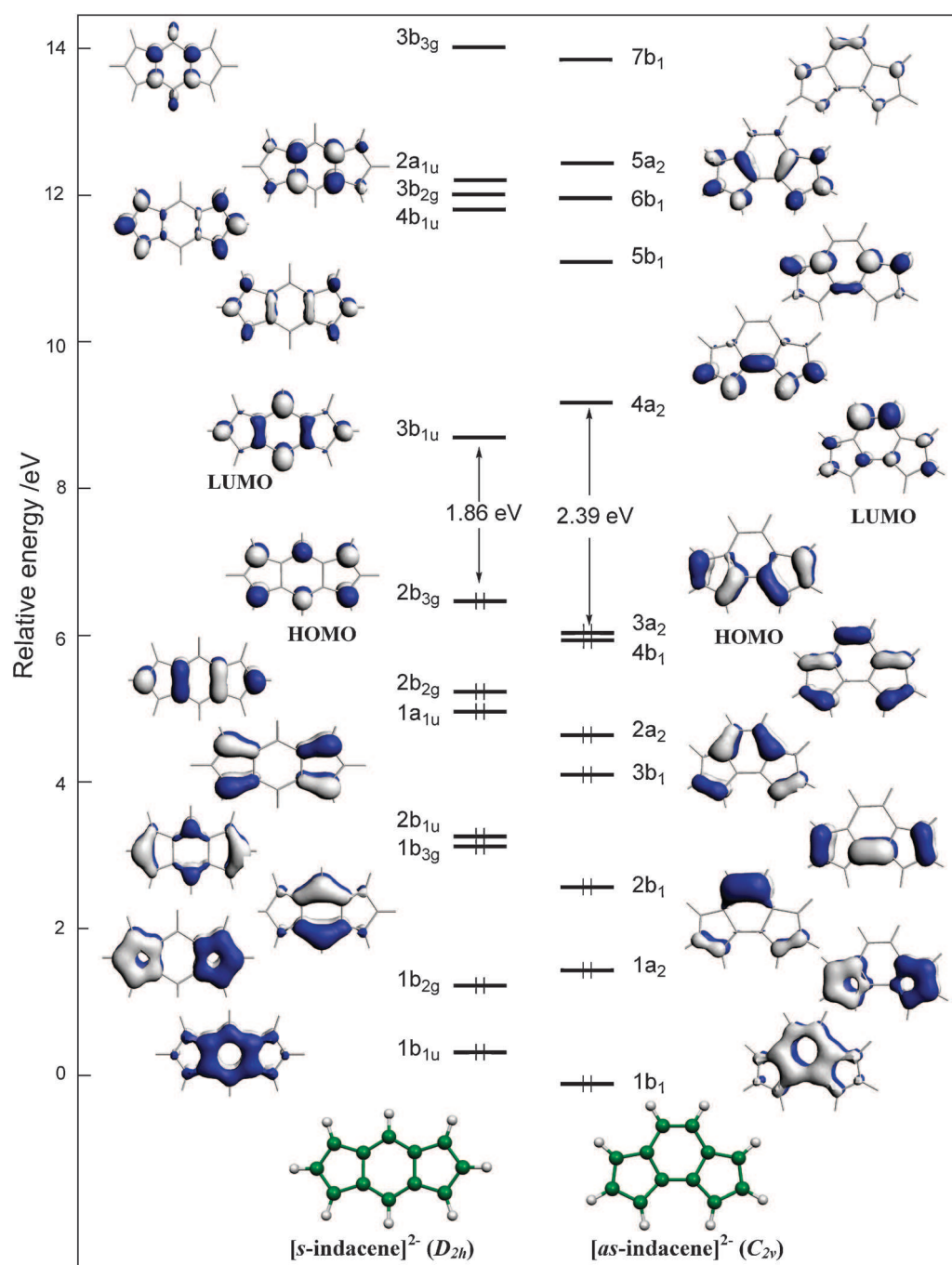


Fig. 1 The π MO diagrams of $[s\text{-indacene}]^{2-}$ and $[as\text{-indacene}]^{2-}$.

38-TNE *syn*- or *anti*-(L_nM) $_2[\eta^5, \eta^5\text{-}(as\text{-Ic}')]$ (Ic' = indacene or any substituted indacene) complexes are known.^{1a,2-4} As expected, the six HOMO's of *anti*-(CpFe) $_2[\eta^5, \eta^5\text{-}(as\text{-Ic})]$ constitute the so-called non-bonding "t_{2g}" block. These non-bonding d-type levels have negligible ligand contribution. The LUMO is an antibonding metal–ligand orbital with significant localization on the conjugated path linking the two C₅ rings of indacene, due to a substantial participation of the LUMO of *as*-Ic (Fig. 1). Going from M = Fe (TNE = 38) to M = Mn (TNE = 36) is mainly equivalent to the removing of two electrons from the weakly metal–metal coupled "t_{2g}" block of the iron species. A weakly coupled

diradical is expected (two 17-electron centers; MVE = 34) without any significant change in the molecular structure, with pentahapto coordination of both metals. Consistently, the energies of the triplet and the broken symmetry (BS) states differ by only 0.03 eV (Table 1). Although the BS geometry does not adopt a perfect C₂ symmetry, its Mulliken spin densities on the metals are equal and they are close to those computed for the triplet state. These results are consistent with the existence of two localized and quasi-independent single electrons, each of them lying on a metal center with very small localization on the *as*-Ic ligand. It should be noted that the BF₄[−] salt of the isoelectronic analog $\{(\text{Cp}^*\text{Fe})_2[\eta^5, \eta^5\text{-}(as\text{-Ic})]\}^{2+}$

Table 1 Relevant computed data for the *anti*-(CpM)₂(*as*-Ic) (M = Mn, Fe, Co, Ni) complexes and their monocations. Unless specified (PBE0 level, cations), the results have been obtained at the BP86 level. Values in brackets are averaged experimental bond distances of the related *anti*-(Cp*Fe)₂(*as*-Ic) complexes (from ref. 5)

M	Mn (TNE = 36)	Fe ⁺ (TNE = 37)	Fe (TNE = 38)	Co ⁺ (TNE = 39)	Co (TNE = 40)	Ni ⁺ (TNE = 41)	Ni (TNE = 42)
Spin state	<i>S</i> = 1	<i>S</i> = 0 (BS ^a)	<i>S</i> = 0	<i>S</i> = 1/2	<i>S</i> = 0	<i>S</i> = 1/2	<i>S</i> = 0
Symmetry	C ₂	C ₁	C ₂	C ₁	C ₂	C ₁	C ₂
<i>syn/anti</i> Relative energy ^b /eV	-0.21	-0.18	-0.28	-0.11	-0.16	-0.08	-0.04
HOMO/LUMO gap in singlet state/eV			1.93	0.30	0.30	0.84	0.84
M/Ic % LUMO in singlet state			45/34	55/16	55/16	35/27	35/27
M/Ic % HOMO in singlet state			57/11	48/26	48/26	44/22	44/22
M/M' spin densities	1.123	-1.084/1.084	0.565/0.565	0.347/0.350	0.782	-0.643/0.643	0.255/0.293
M/M' spin densities (PBE0)		-0.035/1.348	0.066/0.912	0.066/0.912			
M-C(Ic) distances/Å							
M-C(1)/M'-C(8)	2.128	2.161/2.019	2.087/2.087	2.073/2.073	2.055	2.083/2.094	2.142/2.136
M-C(1)/M'-C(8) (PBE0)			2.109/2.098	2.064/2.131			2.132
M-C(2)/M'-C(7)	2.095	2.079/2.073	2.078/2.080	2.074/2.070	2.044	2.064/2.064	2.023/2.017
M-C(2)/M'-C(7) (PBE0)			2.090/2.108	2.062/2.153			1.971
M-C(3)/M'-C(6)	2.121	2.133/2.091	2.099/2.101	2.101/2.099	2.101	2.094/2.083	2.135/2.136
M-C(3)/M'-C(6) (PBE0)			2.113/2.103	2.073/2.132			2.125
M-C(10)/M'-C(9)	2.211	2.267/2.233	2.164/2.163	2.234/2.237	2.358	2.337/2.338	2.500/2.510
M-C(10)/M'-C(9) (PBE0)			2.200/2.098	2.134/2.200			2.654
M-C(11)/M'-C(12)	2.221	2.299/2.296	2.147/2.143	2.142/2.144	2.173	2.298/2.299	2.545/2.553
M-C(11)/M'-C(12) (PBE0)			2.200/2.200	2.152/2.226			2.658

^a BS = broken symmetry calculation. ^b Relative energy of *anti*-(CpM)₂(*as*-Ic) expressed with respect to the ground state of the *syn* configuration.

has been shown to be ferromagnetic with a Curie–Weiss constant of 1.5 K.⁵

Going now from M = Fe (*S* = 0) to M = Co (*S* = 0; TNE = 40) corresponds to formally adding two electrons in an antibonding MO. Thus, a structural reorganization results in order to reduce as much of this antibonding character as possible. The metal atoms move symmetrically away from C(10) and C(9), so that the indacene C₅ rings are now coordinated to the metals in a mode intermediate between pentahapto and tetrahapto, with long Co–C(10) and Co'–C(9) distances (2.358 Å) and still rather long Co–C(11) and Co'–C(12) bonds (2.173 Å). Assuming simple tetrahapto coordination, this symmetrical singlet state is best described as resulting from the coordination of neutral *as*-indacene to neutral CpCo moieties, so that indacene donates four electrons to each Co(II) metal, allowing it to reach the 18-electron configuration (MVE = 36). However, the resulting HOMO/LUMO gap of this singlet state is quite small (0.30 eV). One may anticipate a lower energy minimum which could be either a singlet state with a lower symmetry or a diradical. The possible low symmetry singlet state would be of the type (CpCo)₂[η⁵,η³-(*as*-Ic)], in which one formally Co(III) metal is pentahapto coordinated to indacenediide whereas the other one is a trihapto coordinated Co(I), as sketched on the Lewis formula at the top of Scheme 2. In such a hypothetical structure, each metal center satisfies the 18-electron rule (MVE = 36). It turns out that the singlet state optimized structure of the isoelectronic heteronuclear *anti*-(CpFe)(CpNi)(*as*-Ic) relative exhibits such a coordination mode having a pentahapto Fe(II) center and a trihapto Ni(II) center, but with a small HOMO/LUMO gap of 0.28 eV. However, in the case of the homonuclear di-cobalt species, all our attempts to locate such an unsymmetrical minimum ended up with the previously optimized symmetrical (CpCo)₂(*as*-Ic) singlet state which appears to be the favoured singlet homonuclear structure for this electron count, in agreement also with the fact that the symmetrical broken-symmetry structure is less stable than the triplet state. Thus, this former triplet state was unsurprisingly found to be more stable than its singlet counterpart by 0.05 eV (1.2 kcal mol⁻¹). In this triplet state the Co atoms are also equivalent, but the indacene C₅ rings exhibit strong tendency for trihapto coordination (long Co(10)–C(9)/Co'–C(9) and Co–C(11)/Co'–C(12) bonds), indicative of the existence of two 17-electron centers (MVE = 34). The corresponding broken symmetry state was computed to be less stable than the triplet ground state by 0.08 eV (1.8 kcal mol⁻¹). This small difference in energy is related to the substantial participation of the indacene ligand (*vide supra*) to the singly occupied orbitals. Consistently, the Mulliken spin densities on the metals are much lower than in the case of M = Mn. It should be noted that the BF₄⁻ salt of the related complex (Cp*Co)₂(*as*-Ic) has been shown to be ferromagnetic.⁵ Clearly, both the 40-TNE count and homonuclear nature of this complex favor a triplet ground state associated with a small HOMO/LUMO gap in the corresponding excited singlet state.

Going to M = Ni (TNE = 42) is equivalent to adding one electron in each of the singly occupied orbitals of the triplet ground state of (CpCo)₂(*as*-Ic), thus leading to a singlet ground state for (CpNi)₂(*as*-Ic) with trihapto coordination

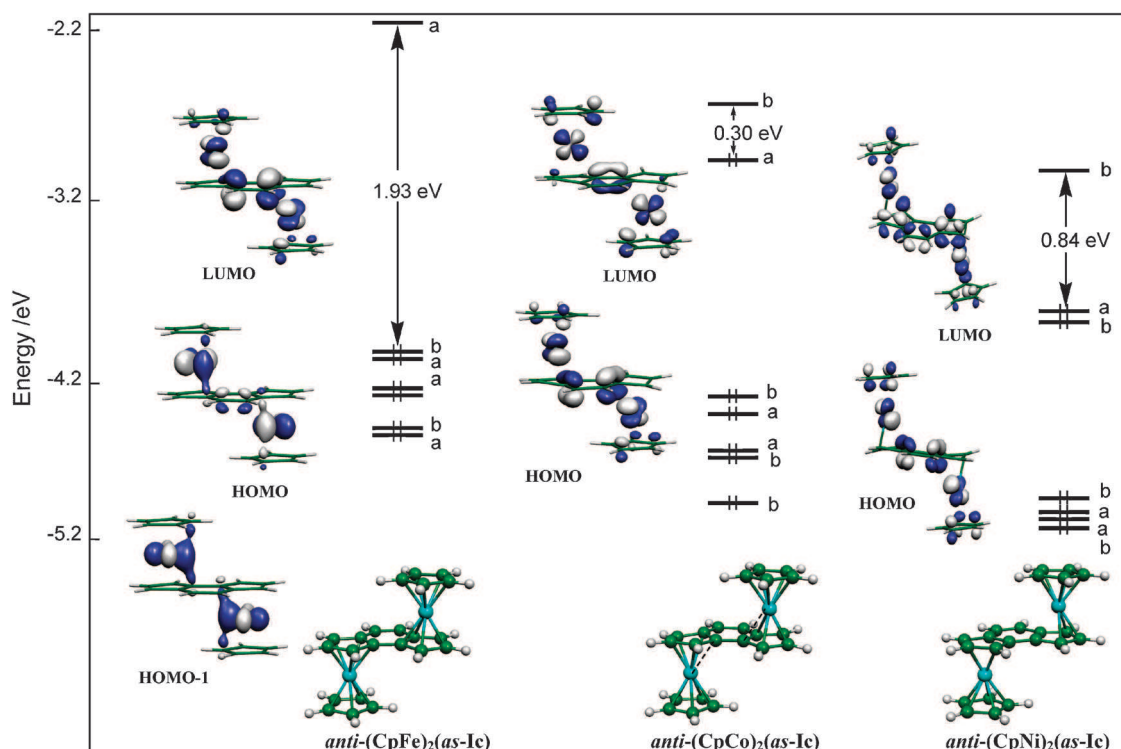


Fig. 2 MO diagrams and frontier orbital plots of the optimized singlet states of the *anti*-(CpM)₂(*as-Ic*) (M = Fe, Co, Ni) complexes (*C*₂ symmetry).

of the indacene C₅ rings. Consistently with the existence of two 18-electron Ni(II) centers (MVE = 36), it is secured by a significant HOMO/LUMO gap (0.84 eV) and the triplet state (not described in Table 1) was found to be less stable by 0.34 eV (7.8 kcal mol⁻¹). This result is in a qualitative agreement with a magnetic susceptibility investigation of (Cp*Ni)₂(*as-Ic*).⁵

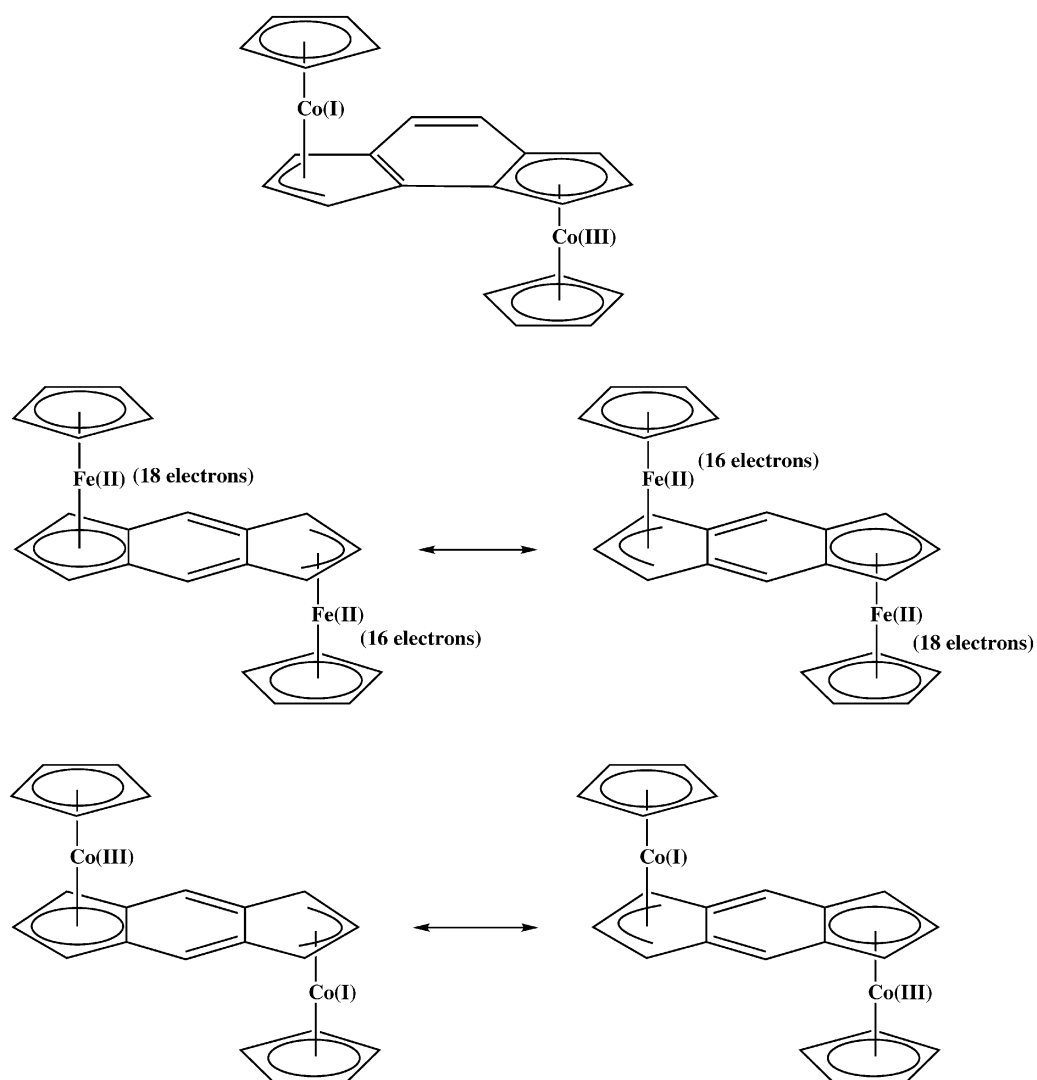
The cationic complexes with TNE counts intermediate between those of the investigated neutral species, *i.e.* those corresponding to M = Fe⁺, Co⁺ and Ni⁺, have also been computed in the *anti* configuration at the same BP86 level as their neutral relatives (Table 1 and Fig. 3). In order to allow the unpaired electron to localize preferentially on one of the two metals, the geometry optimization process was carried out with no symmetry constraint and with unsymmetrical starting geometries. In the three investigated cations, the obtained optimized structures were found to be very close to *C*₂ symmetry, *i.e.* with almost symmetrical metal centers which, consistently, bear almost equal spin densities (Table 1). Consistently with the results obtained for the neutral species, the metal spin density decreases to the benefit of the ligands when going from Fe⁺ to Ni⁺ (see Table 1 and Fig. 3). Since the use of GGA functionals such as BP86 is known for their tendency to favor delocalized mixed valences, we have also optimized the three cations using the PBE0 hybrid functional. The exchange contribution contained in the PBE0 formalism is expected to privilege more localized situations, and indeed this is what happens in the Fe⁺ and Co⁺ cations (Table 1). Unfortunately, unreliable results were obtained in the case of Ni⁺ due to significant spin contamination. In the case of iron both BP86 and PBE0 results are consistent with an

essentially metallic spin density. On the other hand in the case of cobalt, the PBE0 functional favors fully metallic spin density whereas the BP86 functional indicates almost 25% of the ligand contribution into the spin density. Thus, owing to the sensibility of the localized/delocalized nature of the mixed valence with respect to the choice of functional, one may consider these cations as lying on the borderline between Class III (fully delocalized valence) and Class II (situation intermediate between fully localized and fully delocalized valences) using the classification of Robin and Day.¹⁷ Consistently, a salt of the mixed-valence [(CpFe)₂(*as-Ic*)]⁺ cation has been observed averaging its metal centers at the Mössbauer time scale over 100 K.⁵

(CpM)₂(*s-Ic*) complexes

As for the (CpM)₂(*as-Ic*) series, both *syn* and *anti* configurations of the (CpM)₂(*s-Ic*) (M = Mn, Fe, Co, Ni) complexes have been performed at the BP86 level and the *anti* configuration was computed to be the most stable. Since both configurations do not significantly differ electronically, only the *anti* isomers are discussed below. The major computed data and the MO diagrams of the *anti*-(CpM)₂(*s-Ic*) complexes (singlet states) are provided in Table 2 and Fig. 4, respectively.

Starting with the case of M = Fe (TNE = 38), the first question which arises is: how many electrons are donated by the *s-Ic*²⁻ ligand to the CpFe⁺ moieties? Indeed, as said above the *s-Ic*²⁻ is *a priori* ambivalent. If it is best described by structures **I**(*s*) and **I'**(*s*) of Scheme 1 it is a 12-electron donor and consequently (CpFe)₂(*s-Ic*) is a 36-MVE species satisfying the octet rule. On the other hand, if it is best described by



Scheme 2

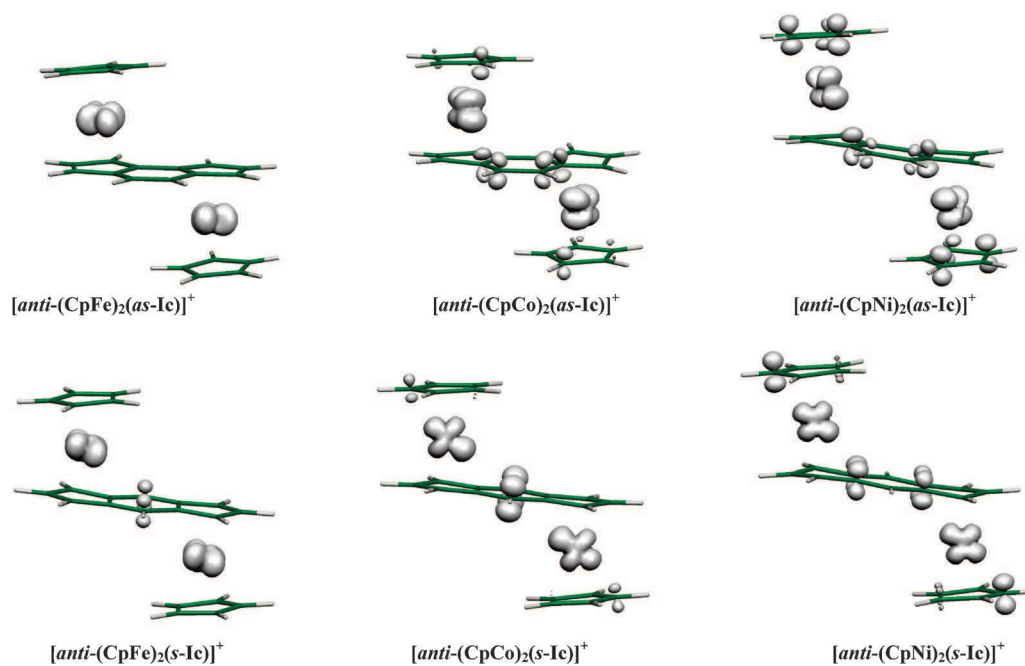


Fig. 3 Mulliken spin densities of $[anti-(CpM)_2(as-Ic)]^+$ and $[anti-(CpM)_2(s-Ic)]^+$ ($M = Fe, Co, Ni$; BP86 calculations).

Table 2 Relevant computed data for the *anti*-(CpM)₂(s-Ic) (M = Mn, Fe, Co, Ni) complexes and their monocations. Unless specified (cations), the results have been obtained at the BP86 level. Values in brackets are averaged experimental bond distances of related *anti*-(Cp*M)₂(s-Ic) complexes (from ref. 5)

M	Mn (TNE = 36)	Fe ⁺ (TNE = 37)	Fe (TNE = 38)	Co ⁺ (TNE = 39)	Co (TNE = 40)	Ni ⁺ (TNE = 41)	Ni (TNE = 42)
Spin state	S = 0	S = 1	S = 0	S = 1/2	S = 0	S = 0	S = 1
Symmetry	C _{2h}	C _{2h}	C _{2h}	C _s	C _{2h}	C _s	C ₁
<i>syn/anti</i> Relative energy ^b /eV	0.10	-0.13	-0.16	-0.05	-0.01	0.09	0.07
<i>s</i> (as relative energy ^c /eV)	0.25	0.72	0.74	0.90	0.33	0.33	0.07
HOMO/LUMO gap (eV) in singlet state	0.60	43/33	52/24	52/21	0.277/0.275	0.781/0.460	0.000/0.000
M/Ic % LUMO in singlet state	69/28	71/26	0.362/0.348	0.626/0.549	2.118/2.119	2.158	2.160/2.194 [2.069]
M/Ic % HOMO in singlet state	91/01	1.113	1.131/1.129	0.490/0.480	2.072 [2.046]	2.008	1.990/2.045 [1.965]
M/M' spin densities	—	1.113	1.131/1.129	0.490/0.480	2.061 [2.036]	2.589	2.543/2.640 [2.470]
M/M' spin densities (PBE0)	—	1.113	1.131/1.129	0.490/0.480	2.196 [2.133]	2.663	2.663/2.662
M-C(1c) distances/Å:	—	1.113	1.131/1.129	0.490/0.480	2.240/2.259	—	—
M-C(1)/M'-C(5)	2.104	2.1171	2.114/2.114	2.084/2.086	2.074/2.071	2.158	2.160/2.194 [2.069]
M-C(1)/M'-C(5) (PBE0)	2.111	2.089	2.092/2.091	2.113/2.087	2.073/2.077	2.008	1.990/2.045 [1.965]
M-C(2)/M'-C(6)	2.145	2.260	2.236/2.236	2.168/2.173	2.039/2.040	2.589	2.543/2.640 [2.470]
M-C(2)/M'-C(6) (PBE0)	—	—	—	—	2.055/2.056	—	—
M-C(9)/M'-C(12)	—	—	—	—	2.273/2.263	—	—
M-C(9)/M'-C(12) (PBE0)	—	—	—	—	2.240/2.259	—	—

^a BS = broken symmetry calculation. ^b Relative energy of *anti*-(CpM)₂(s-Ic) expressed with respect to the ground state of the *syn* configuration. ^c Relative energy of the ground state of *anti*-(CpM)₂(s-Ic) expressed with respect to the ground state of its *anti*-(CpM)₂(as-Ic) isomer described in Table 1.

structures **III**(s), **III'**(s) or **IV**(s), it is an electron-deficient 34-MVE species. The computed HOMO/LUMO gap (0.74 eV) of *anti*-(CpFe)₂(as-Ic) is moderate, much smaller than that of its 36-MVE *anti*-(CpFe)₂(s-Ic) isomer (1.93 eV) and that of free *s*-Ic²⁻ (2.11 eV). The LUMO of *anti*-(CpFe)₂(s-Ic) has a substantial participation of the LUMO of *s*-Ic²⁻ (~30%), the HOMO is mainly 3d(Fe) in character. Thus the HOMO and LUMO of (CpFe)₂(s-Ic) are not strongly correlated to the HOMO and LUMO of free *s*-Ic²⁻ and the lower HOMO/LUMO gap of the former is not a consequence of a largest statistical weight of structures **III**(s), **III'**(s) or **IV**(s) of the latter upon coordination. Consistently, the triplet state of *anti*-(CpFe)₂(s-Ic) is found to lie significantly above the singlet ground state (by 0.37 eV). Thus, (CpFe)₂(s-Ic) is best described as a stable diamagnetic 34-MVE “unsaturated” species. We have shown previously that this electron count favors closed-shell stability in the case of dinuclear complexes of fused conjugated polycyclic ligands such as pentalene or azulene.¹⁶ The reason lies in the fact that the formal “electron deficiency” is associated with a vacant non-bonding combination of metal AO's which is too high in energy for being electron-accessible, due to its large metal valence s and p (and small d) character. The same situation occurs in (CpFe)₂(s-Ic). Indeed, assuming that *s*-Ic²⁻ is a 10-electron donor best described by formulae **I**(s) and **I'**(s) of Scheme 1, two ligand π -type electron pairs do not participate in the bonding with the metals. From symmetry arguments one can deduce that they should lie in b_g and b_u MO's. Thus, one is left with 5 π -type donor MO's spanning 2 \times a_g + b_g + a_u + b_u on *s*-Ic²⁻ and 6 vacant accepting hybrid combinations¹⁸ spanning 2 \times a_g + b_g + a_u + 2 \times b_u on the (CpFe...FeCp)²⁺ fragment. In the simplified picture of a one-to-one interaction diagram sketched in Fig. 5, one is left with one high-lying non-bonding hybrid combination of b_u symmetry. In this simplified view, the rather low-lying π^* LUMO of *s*-Ic²⁻ (see Fig. 1) is expected to be the (CpFe)₂(s-Ic) LUMO and the six “t_{2g}” non-bonding occupied combinations¹⁸ of (CpFe...FeCp)²⁺ should be the highest occupied levels of (CpFe)₂(s-Ic). The resulting HOMO/LUMO gap is significant, but not very large due to the rather low energy of the π^* LUMO of *s*-Ic²⁻. Although this approximate description does not account for the mixing of the π^* LUMO of *s*-Ic²⁻ with the metallic orbitals, nor the mixing of the metallic “t_{2g}” combinations with the π levels of *s*-Ic²⁻ (compare Fig. 4 and 5), it contains enough information for providing a satisfying qualitative rationalization of the computed electronic structure of (CpFe)₂(s-Ic). Thus (CpFe)₂(s-Ic) is deficient by two electrons with respect to the 18-electron rule, the deficiency being equally delocalized on both metals which are best described as 18/16-MVE (not 17-MVE) centers, as sketched in the middle of Scheme 2. This description is consistent with the fact that the pentahapto coordination mode of the Fe atoms is somewhat distorted towards a trihapto one (see Table 2) which would correspond to a pseudo-square planar coordination mode. These results are also consistent with the X-ray structure and diamagnetic behavior of (Cp*Fe)₂(s-Ic).⁵ Related dinuclear complexes of substituted pentalenes also exhibit similar structures in the solid state.⁶⁻⁹

The HOMO of (CpFe)₂(s-Ic) derives from a “t_{2g}” combination which is mixed in a substantial antibonding way with

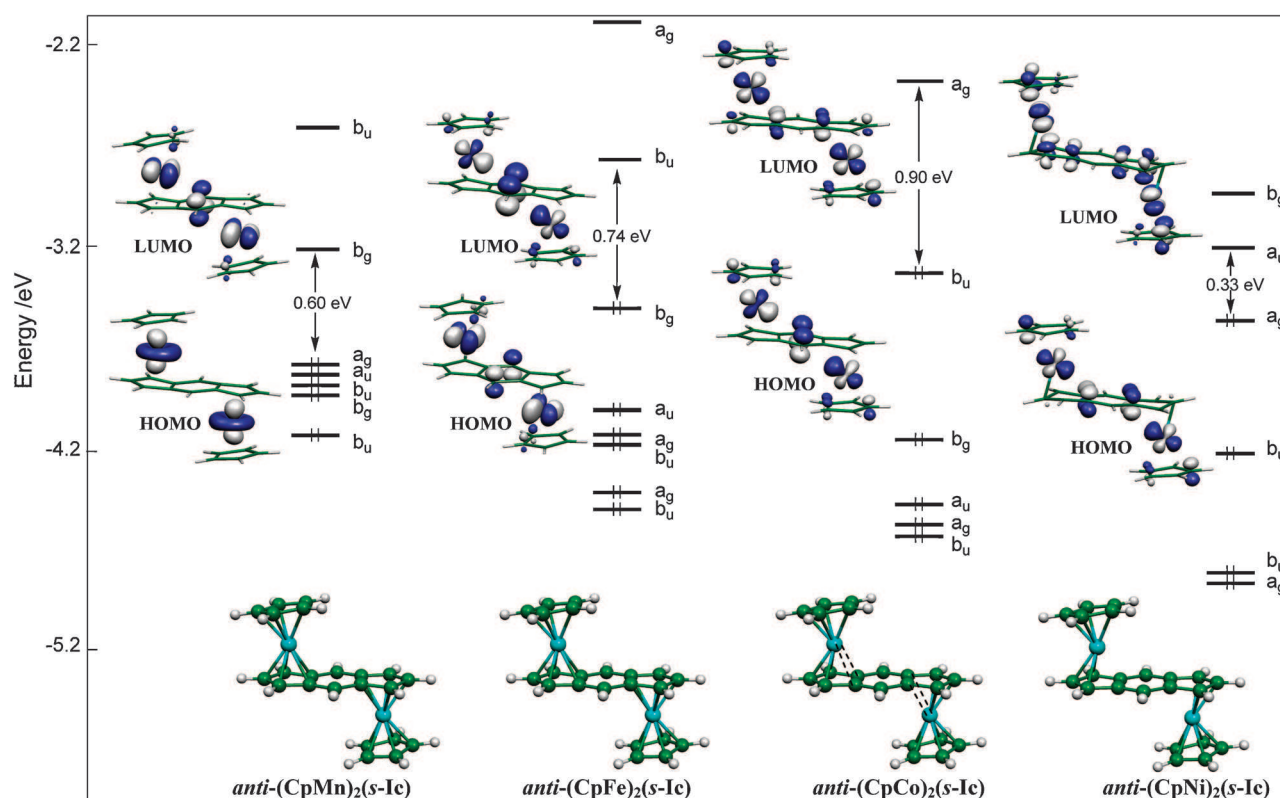


Fig. 4 MO diagrams and frontier orbital plots of the optimized singlet states of the *anti*-(CpM)₂(s-Ic) (M = Mn, Fe, Co, Ni) complexes (*C*_{2h} symmetry).

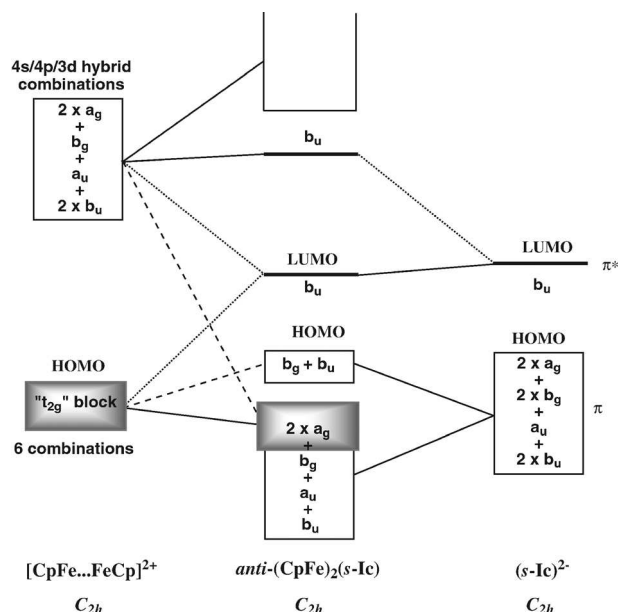


Fig. 5 Simplified MO interaction diagram for the 38-TNE complex *anti*-(CpFe)₂(s-Ic).

the Ic²⁻ HOMO so that it is somewhat higher in energy than the other “t_{2g}” combinations. Removing two electrons from this HOMO leads to a closed-shell situation, which is secured by a moderate HOMO/LUMO gap of 0.60 eV in the singlet state of the 36-TNE (CpMn)₂(s-Ic) complex. This is a highly electron-deficient species, but due to the delocalized nature of

its LUMO (HOMO of (CpFe)₂(s-Ic)), the electron deficiency is shared by the indacene ligand. This singlet state is however less stable than its corresponding triplet state by 0.23 eV (5.3 kcal mol⁻¹), in agreement with the fact that the isoelectronic [(Cp*Fe)₂(s-Ic)]²⁺ has been reported to have a triplet ground state,⁵ but not considering that the energy of the corresponding broken symmetry state of (CpMn)₂(s-Ic) is found 0.07 eV (1.6 kcal mol⁻¹) below that of the triplet state. Nevertheless, this energy difference is quite small. The broken symmetry spin densities are very similar to those of the triplet state, indicating weak coupling between the unpaired electrons.

Adding two electrons to (CpFe)₂(s-Ic) leads to a closed-shell situation because, for the reasons described above, its b_u LUMO lies isolated in a large energy gap (see Fig. 4 and 5). Thus, the 40-TNE (CpCo)₂(s-Ic) complex has a singlet ground state, secured by a substantial HOMO/LUMO gap of 0.90 eV. However, the coordination mode of (CpCo)₂(s-Ic) is somewhat different from that of (CpFe)₂(s-Ic) and (CpMn)₂(s-Ic). Whereas in the two latter complexes the metal atoms coordinate the C₅ rings in a pentahapto fashion, the long M–C(9) and M'–C(12) bonds of 2.328 Å in the former indicate a coordination mode intermediate between pentahapto and trihapto. Thus, (CpCo)₂(s-Ic) is best described by the mesomeric Lewis structures sketched at the bottom of Scheme 2, in which both metals reach the 18-electron count (MVE = 36). The search for an unsymmetrical structure corresponding to one of the Lewis structure of Scheme 2 did not succeed. It is noteworthy that the isoelectronic complexes *anti*-(Cp*Co)₂(s-Ic)⁵ and *syn*-(CpCo)₂(Bu'₄-s-Ic)⁸ have been reported to be diamagnetic

and that *syn*-[Fe(CO)₃]₂(Bu^t₄-*s*-Ic)⁹ exhibits in the solid state a trihapto coordination mode similar to that computed in our *anti*-(CpCo)₂(*s*-Ic) model, but somewhat distorted, presumably for steric reasons.

With two more electrons, the singlet state of (CpNi)₂(*s*-Ic) (TNE = 42) exhibits two trihapto metals bonding the indacene ligand, *i.e.* satisfying the 18-electron rule. Its geometry exhibits similar metrical data as the X-ray structure of (Cp*Ni)₂(*s*-Ic).⁵ However, its computed HOMO/LUMO gap (0.33 eV) is small and the triplet state is computed to be more stable by 0.10 eV (2.3 kcal mol⁻¹). Optimizing this triplet state under C_{2h} symmetry constraint results in a small computed imaginary frequency of 40i cm⁻¹ which disappears when releasing the symmetry to C_s, although the total energy remains virtually unchanged. This situation is indicative of a very flat potential energy surface around the minimum. Nevertheless, the optimized C_s structure exhibits rather similar trihapto coordination modes as in the optimized singlet and C_{2h} triplet structures but shows unsymmetrical spin density distribution on the Ni atoms (Table 2). The corresponding broken symmetry state is computed to be 0.07 eV (1.6 kcal mol⁻¹) higher in energy and surprisingly exhibits almost no metallic spin density, the latter being essentially distributed on the indacene ligand. These differences between the triplet and broken symmetry states indicate significant coupling between the unpaired electrons in the triplet ground state. It should be noted that the related (Cp*Ni)₂(*s*-Ic) complex has been reported to be antiferromagnetic with a very small singlet/triplet splitting (1.3 kcal mol⁻¹).⁵

The cationic complexes of Fe, Co and Ni were also investigated, both at the BP86 and PBE0 levels. The major results are provided in Table 2 and Fig. 3. As for [(CpNi)₂(*as*-Ic)]⁺, the [(CpNi)₂(*s*-Ic)]⁺ results were found unreliable due to large spin contamination. For the BP86 results the same tendency as in the *s*-Ic series was found in the *as*-Ic series, that is, spin delocalization with a lowering of the metal participation to the spin density when going from Fe⁺ to Ni⁺. On the other hand, the PBE0 results show a dominant metal participation to the spin density in both Fe⁺ and Co⁺ cations, with localization on one metal center in the case of Fe⁺ and delocalization on both metals in the case of Co⁺, in contrast to what was found in the related [(CpCo)₂(*as*-Ic)]⁺ (see above).

Concluding remarks

Within the (CpM)₂(*as*-Ic) series, strong stability is obtained for the TNE electron count of 38 (M = Fe) for which a very large HOMO/LUMO gap is associated with the existence of two 18-electron centers (MVE = 38). Whereas removing two electrons (MVE = 36) generates two almost independent unpaired electrons, the successive addition of supplementary electrons results in the population of antibonding metal–indacene orbitals, leading to partial metal–indacene decoordination and minor but significant participation of ligand spin density (TNE = 39–41). Only the TNE = 42 (M = Ni) count favors a closed-shell ground state and 18-electron configuration for each metal center (MVE = 38). Within the (CpM)₂(*s*-Ic) series, the 38-TNE count also favors a closed-shell ground-state, although the two metal atoms as a whole lack two electrons

for each of them reaching the 18-electron configuration. Removing two electrons (MVE = 36) generates an electron deficient species which has a diradicalar ground state. On the other hand, the closed-shell MVE = 38 situation is found only for TNE = 40 (M = Co). The open-shell configurations corresponding to TNE = 39, 41 and 42 indicate more metal–metal communication than in the *as*-Ic series. Nevertheless, all the computed mixed-valent species can be classified as lying in the borderline between Class II and Class III.¹⁷ Finally, one should mention that the possibility of coordinating the C₆ ring of indacene to one of the two metal atoms has also been tested, both in the *syn* and *anti* configurations, the former allowing the formation of metal–metal bonding. All the computed structures were found to have much higher energies than those reported in Tables 1 and 2 and thus are not discussed in this article.

Computational details

Calculations were carried out within the formalism of the density functional theory (DFT) with the Amsterdam Density Functional package (ADF 2007.01).¹⁹ All the investigated models were computed using the VWN local density parameterization,²⁰ with the generalized gradient BP86 functional.²¹ In the case of the mixed-valent cationic complexes, calculations were also carried out with the PBE0 hybrid functional²² for the sake of comparison (see text). In the particular cases of PBE0 calculations on the Ni cations, significant spin contamination was obtained, leading us to disregard these results. The analytical gradient method implemented by Verluis and Ziegler was used.²³ The standard ADF TZP atomic basis set was used, *i.e.*, triple- ζ STO basis set for H 1s (augmented with a 2p single- ζ polarization function), for C 2s and 2p (augmented with a 3d single- ζ polarization function), and triple- ζ STO basis set for Mn, Fe, Co and Ni 3d and 4s (augmented with a single- ζ 4p polarization function). The frozen-core approximation was used to treat the core shells up to 1s for C, N and O and 3p for Mn, Fe, Co and Ni.¹ Spin-unrestricted calculations were performed for all the open-shell systems. Vibrational frequency calculations²⁴ were performed on all the studied compounds to check that the optimized structures are minima on the potential energy hypersurface. Representations of the molecular orbitals and spin densities were done using the MOLEKEL²⁵ program.

Acknowledgements

This research has been performed as part of the Chilean-French «Joint Laboratory for Inorganic Functional Materials» (LIA MIF No. 836). Computing facilities were provided by the IDRIS-CNRS Center (France). FONDECYT Grants 1100283, 1110758, 1110902 have supported part of this research. Financial support from the University of Rennes I, the CNRS and the Institut Universitaire de France (J.-Y. S.) is gratefully acknowledged.

References

- (a) S. Barlow and D. O'Hare, *Chem. Rev.*, 1997, **97**, 637; (b) A. Ceccon, S. Santi, L. Orian and A. Bisello, *Coord. Chem. Rev.*, 2004, **248**, 683; (c) P. Aguirre-Etcheverry and D. O'Hare, *Chem. Rev.*, 2010, **110**, 4839.

- 2 W. L. Bell, C. J. Curtis, A. Miedaner, C. W. Eigenbrot Jr, R. C. Haltiwanger, C. G. Pierpont and J. C. Smart, *Organometallics*, 1988, **7**, 691.
- 3 P. Ganis, A. Ceccon, T. Kohler, F. Manoli, S. Santi and A. Venzo, *Inorg. Chem. Commun.*, 1998, **1**, 15.
- 4 A. Ceccon, A. Bisello, L. Crociani, A. Gambaro, P. Ganis, F. Manoli, S. Santi and A. Venzo, *J. Organomet. Chem.*, 2000, **600**, 94.
- 5 J. M. Manriquez, M. D. Ward, W. M. Reiff, J. C. Calabrese, N. L. Jones, P. J. Carroll, E. E. Bunel and J. S. Miller, *J. Am. Chem. Soc.*, 1995, **117**, 6182.
- 6 W. L. Bell, C. J. Curtis, C. W. Eigenbrot Jr, C. G. Pierpont, J. L. Robbins and J. C. Smart, *Organometallics*, 1987, **6**, 266.
- 7 M. Sato, M. Suzuki, M. Okoshi, M. Kurasina and M. Watanabe, *J. Organomet. Chem.*, 2002, **648**, 72.
- 8 P. Roussel, M. J. Drewitt, D. R. Cary, C. G. Webster and D. O'Hare, *Chem. Commun.*, 1998, 2205.
- 9 D. R. Cary, C. G. Webster, M. J. Drewitt, S. Barlow, J. C. Green and D. O'Hare, *Chem. Commun.*, 1997, 953.
- 10 P. Roussel, D. R. Cary, S. Barlow, J. C. Green, F. Varret and D. O'Hare, *Organometallics*, 2000, **19**, 1071.
- 11 M. T. Garland, J.-Y. Saillard, I. Chávez, B. Oëlckers and J. M. Manriquez, *THEOCHEM*, 1997, **390**, 199–208.
- 12 (a) D. MacLeod Carey, C. Morales-Verdejo, A. Munoz-Castro, F. Burgos, D. Abril, C. Adams, E. Molins, O. Cador, I. Chavez, J. M. Manriquez, R. Arratia-Perez and J.-Y. Saillard, *Polyhedron*, 2010, **29**, 1137; (b) A. Munoz-Castro, D. MacLeod Carey, C. Morales-Verdejo, I. Chavez, J. M. Manriquez and R. Arratia-Perez, *Inorg. Chem.*, 2010, **49**, 4175.
- 13 L. Orian, P. Ganis, S. Santi and A. Ceccon, *J. Organomet. Chem.*, 2005, **690**, 482.
- 14 S. Santi, L. Orian, C. Durante, E. Z. Bencze, A. Bisello, A. Donoli, A. Ceccon, F. Benetollo and L. Crociani, *Chem.–Eur. J.*, 2007, **13**, 7933.
- 15 S. Santi, L. Orian, A. Donoli, C. Durante, A. Bisello, M. Di Valentin, P. Ganis, F. Benetollo and A. Ceccon, *J. Organomet. Chem.*, 2008, **693**, 3797.
- 16 (a) S. Bendjaballah, S. Kahlal, K. Costuas, E. Bévilion and J.-Y. Saillard, *Chem.–Eur. J.*, 2006, **12**, 2048; (b) H. Korichi, F. Zouchoune, S.-M. Zendaoui, B. Zouchoune and J.-Y. Saillard, *Organometallics*, 2010, **29**, 1693.
- 17 M. B. Robin and P. Day, *Adv. Inorg. Chem. Radiochem.*, 1967, **10**, 24.
- 18 T. A. Albright, J. K. Burdett and M. H. Whangbo, *Orbital Interactions in Chemistry*, John Wiley and Sons, New York, 1985.
- 19 (a) G. te Velde, F. M. Bickelhaupt, C. Fonseca Guerra, S. J. A. van Gisbergen, E. J. Baerends, J. G. Snijders and T. Ziegler, *J. Comput. Chem.*, 2001, **22**, 931; (b) C. Fonseca Guerra, J. G. Snijders, G. te Velde and E. J. Baerends, *Theor. Chem. Acc.*, 1998, **99**, 391; (c) *ADF2007.01, Theoretical Chemistry*, Vrije Universiteit, Amsterdam, The Netherlands, SCM, www.scm.com.
- 20 S. D. Vosko, L. Wilk and M. Nusair, *Can. J. Phys.*, 1980, **58**, 1200.
- 21 (a) A. D. Becke, *Phys. Rev. A: At., Mol., Opt. Phys.*, 1988, **38**, 3098; (b) J. P. Perdew, *Phys. Rev. B*, 1986, **33**, 8822.
- 22 (a) S. Grimmes, *J. Comput. Chem.*, 2004, **25**, 1463; (b) M. Ernzerhof and G. Scuseria, *J. Chem. Phys.*, 1999, **110**, 5029; (c) C. Adamo and V. Barone, *J. Chem. Phys.*, 1999, **110**, 6158.
- 23 L. Verluise and T. Ziegler, *J. Chem. Phys.*, 1988, **88**, 322.
- 24 (a) L. Fan and T. Ziegler, *J. Chem. Phys.*, 1992, **96**, 9005; (b) L. Fan and T. Ziegler, *J. Phys. Chem.*, 1992, **96**, 6937.
- 25 P. Flükiger, H. P. Lüthi, S. Portmann and J. Weber, *Molekel 4.1*, Swiss Center for Scientific Computing, Manno, 2002.